# Research into Power and Load Parameters of Flexible Screw Conveyors for Transportation of Agricultural Materials

**Volodymyr Bulgakov, Simone Pascuzzi, Valerii Adamchuk, Jüri Olt, Zinovii Ruzhylo, Oleksandra Trokhaniak, Francesco Santoro, Margus Arak, Janusz Nowak, and Hristo Beloev**

**Abstract** In order to carry out experimental research and determine the performance criteria for the transportation of agricultural materials, a test unit of the combined screw conveyor has been designed by the authors. The axial speed and capacity of bulk material transportation on a curved route have been determined for the articulated-section operating device of the screw conveyor. The calculation has proved that the angular velocities of adjacent sections are almost the same. As a result of the research into the power and load parameters of flexible screw conveyors, graphic relations between the values of the torque T and power N, on the one hand, and the rate of rotation of the operating device's drive shaft, on the other hand, have been plotted for the process of transportation of bulk materials in screw conveyors, when the process pipeline is fully filled with grain material.

**Keywords** Agricultural material · Screw conveyor · Transportation

V. Bulgakov · Z. Ruzhylo · O. Trokhaniak
National University of Life and Environmental Sciences of Ukraine, Kyiv, Ukraine

S. Pascuzzi (✉) · F. Santoro
Department of Agricultural and Environmental Science, University of Bari Aldo Moro, Bari, Italy
e-mail: simone.pascuzzi@uniba.it

V. Adamchuk
Institute of Mechanics and Automation of Agricultural Production of the National Academy of Agrarian Sciences of Ukraine, Glevakha, Vasylkiv Dist., Kyiv Region, Ukraine

J. Olt · M. Arak
Institute of Forestry and Engineering, Estonian University of Life Sciences, 56 Kreutzwaldi Str., 51006 Tartu, EE, Estonia

J. Nowak
Department of Operation of Machines and Management of Production Processes, University of Life Sciences in Lublin, 13, Akademicka Str., 20-950 Lublin, Poland

H. Beloev
Department of Agricultural Machinery, University of Ruse Angel Kanchev, BG 7017 Ruse, Bulgaria



S. Pascuzzi and F. Santoro (eds.), *Farm Machinery and Processes Management in Sustainable Agriculture*, Lecture Notes in Civil Engineering 289,
https://doi.org/10.1007/978-3-031-13090-8_6

## 1 Introduction

Flexible screw conveyors are widely used in the transportation of agricultural materials in various production processes and efficiently perform the functions required from them [1]. However, the existing screw-type operating devices cannot fully meet the performance requirements to such types of conveyors [2]. Continuous auger flights quickly deteriorate due to the action of alternating cyclic loads, while the combined and sectioned operating devices are material-intensive parts. Their operation results in the increased consumption of power and heavy wear of the inner surfaces of the flexible casings [3, 4].

The completed theoretical and experimental investigations on the conditions in the zones of the loading and transhipment of bulk agricultural materials in case of single- and double-line screw conveyors as well as the intake of the materials by active loading spouts have provided for selecting the rational design, kinematic and dynamic parameters of the operating devices as well as their operating conditions [5–7].

In the papers [4, 8], the parameters and operating conditions are determined for vertical and inclined screw conveyors transporting agricultural materials and the rational parameters are established for their operating devices. The results of the research into the motion of materials in screw conveyors with rotary casings are presented in the paper [9].

The development and analysis of screw conveyors as well as their contribution to the damaging of materials are discussed in the papers [10].

In view of the above-said, it is necessary to improve the existing and develop new designs of auger operating devices for screw conveyors, determine their optimum design and kinematic parameters that would provide for raising their performance in the process of transporting agricultural materials.

The application of swivel-joint screw operating devices can ensure high efficiency in the performance of loading/discharge processes in the transportation of bulk agricultural materials on curved routes.

The aim of the research was to raise the performance efficiency of flexible screw conveyors in the transportation of agricultural materials by way of developing new auger-type operating devices.

## 2 Materials and Methods

In order to improve the performance of screw conveyors, the authors have developed the design of a sectioned shaft with a radial ball connection between the sections

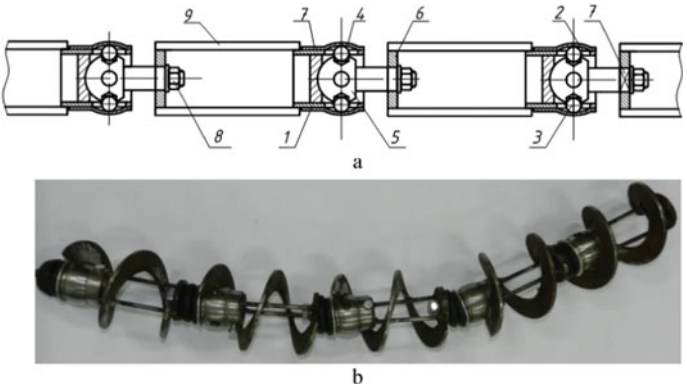


**Fig. 1** Structural layout of articulated shaft **a** and picture of articulated-section screw operating device **b**

(Fig. 1). At the right end of each section, the cylindrical bushing 1 is fixed. The latter has a system of parallel slots 2, which are placed with equal spacing on the circumference and interface the rolling elements 3. On the other side, the rolling elements 3 are contained in the inner spherical surface of the bushing 4, which enables the swivelling rotation of the spherical pivot 5.

On the opposite side of each section, inside its left end, the connecting bushing 6 equipped with the square or profiled hole 7 is rigidly installed normally to the centreline of the section. The respective end of the spherical pivot 5 from the adjacent section is inserted into the hole 7 and rigidly fixed in it with the nut 8. On the outer circumference of the connecting bushing 6, the linking rods 9 are rigidly fixed with equal spacing. The opposite ends of the linking rods 9 are connected to the outer surface of the bushing 1. Onto each cylindrical section, a screw section is attached (Fig. 1).

When a section of the auger is rotated, the rotational motion is transferred via the rolling elements 3 to the spherical pivot 5 and to the adjacent screw sections.

In order to analyse the process of the bulk material transportation by the screw conveyor with an articulated-section screw operating device, the axial velocity of the bulk material in a horizontal high-speed screw conveyor is determined with the use of the following relation [11–13]:

$$V_{ax} = \frac{T_s(\omega - \omega_k)}{2\pi} \tag{1}$$

where $T_s$ – lead of helix; $\omega$ – angular velocity of the bulk material; $\omega_k$ – angular velocity of the circumferential component of motion of the bulk material. The relation (1) can be represented in the following form:

$$V_{ax} = \frac{T_s\omega}{2\pi} \cdot k_v$$

where

$$k_v = \frac{k_s}{tan\,\theta\, tan(\theta + \varphi) + 1}, \tag{2}$$

where: $\theta$ – angle of lead of the section helix; $\varphi$ – friction angle of the bulk material with respect to the surface of the helix, where $\varphi = arctan\,\mu_1$; $\mu_1$- friction factor; $k_s$ – coefficient that represents the design solution of the sectioned screw conveyor, $k_s$ = 0.98–0.99.

In case the bulk material is transported at an angle of $\alpha$ to the horizontal surface, its axial velocity is reduced, which is taken into account with the coefficient $k_\alpha$:

$$V_{ax\alpha} = V_{ax} \cdot k_\alpha. \tag{3}$$

In case the sectioned screw conveyor is positioned vertically [14–16]:

$$k_\alpha = 1 - S_c = 1 - \frac{\omega_k}{\omega} = 1 - \sqrt{\frac{tan(\theta + \varphi)}{\mu_2 \rho}} \tag{4}$$

where $S_c$ – coefficient of dynamic similarity; $\rho$ – power-speed coefficient, $\rho = \frac{\omega^2 R_c}{g}$; $R_c$ – external radius of helix, $g$ – acceleration of gravity, $g = 9.81$ m s$^{-2}$.

Accordingly, the axial transportation velocity of the bulk material in the vertical part of the flexible screw conveyor is equal to:

$$V_{axB} = \frac{T_s \omega}{2\pi} \cdot \frac{k_s\left[1 - \sqrt{\frac{g\, tan(\theta+\varphi)}{\omega^2 \mu_2 R_c}}\right]}{tan\,\theta\, tan(\theta + \varphi) + 1}. \tag{5}$$

In case of a flexible conveyor, in which the route turns in space, but the loading is done in the horizontal direction, under the condition of maintaining a constant capacity of $Q = const$ along the route, the coefficient of charge $\psi$ at the loading point has to take into account its changing as a result of the changes in the axial velocity of transportation [17]:

$$\psi_o V_o = \psi_\alpha V_\alpha. \tag{6}$$

Therefore, the amount of the change in $V_\alpha$ on the transportation route is extremely important. The change in the axial velocity of transportation can be approximated by the parabola of the following form:

$$V_\alpha = V_h - (V_h - V_w)\left(\frac{2\alpha}{\pi}\right)^\lambda, \tag{7}$$

where $V_h$ and $V_w$ – horizontal and vertical components of the transportation velocity, respectively. for $\alpha = 90°$ we can write $V_w = V_h \cdot k_\alpha$.

Taking into account the expression (4),

$$V_\alpha = V_h\left[1 - S_c\left(\frac{2\alpha}{\pi}\right)^\lambda\right]; \tag{8}$$

or

$$V_\alpha = V_h\left[1 - \frac{1}{\omega}\sqrt{\frac{g\,tan(\theta+\varphi)}{\mu_2 R_c}}\left(\frac{2\alpha}{\pi}\right)^\lambda\right] \tag{9}$$

where the parameter $\lambda$ depends on the rheological properties of the bulk material and to a first approximation can be assumed to be equal to $\lambda = 2$. Therefore, the curve presented in expression (9) can be considered a parabola and the dependence of the velocity $V_\alpha$ on the angle $\alpha$ can, in the first approximation, be considered parabolic.

In the case of a freely suspended screw conveyor, the centreline of the flexible auger has the form of a catenary line, which varies according to the following relation:

$$y = a\left(ch\frac{x}{a} - 1\right), \tag{10}$$

where the parameter $a$ depends on the elevation of the discharge end opening and can be determined from the following relation:

$$\frac{h}{a} + 1 = ch\left(\frac{l_x}{a}\right), \tag{11}$$

where $h$ – elevation; $l_x$ – horizontal projection of the conveyor length.

The current angle of pipeline inclination is determined by the following relation:

$$tan\,\alpha = \frac{dy}{dx} = sh\frac{x}{a}, \tag{12}$$

whence

$$\alpha = arctan\left(sh\frac{x}{a}\right). \tag{13}$$

Hence, in case of a freely suspended flexible (sectioned) screw conveyor, the axial velocity of the bulk material transportation is equal to:

$$V_{ax\alpha} = V_h\left[1 - \frac{1}{\omega}\sqrt{\frac{g\,tan(\theta+\varphi)}{\mu_2 R_c}}\left(\frac{2\,arctan\left(sh\frac{x}{a}\right)}{\pi}\right)^\lambda\right]. \tag{14}$$

The coefficient of charge $\psi_\alpha$ in the most unfavourable cross-section may not exceed $\psi_\alpha \leq 0.7$. Accordingly, in the loading area, the rational coefficient of charge has, in accordance with (6), to be equal to:

$$\psi_o = \frac{\psi_\alpha V_\alpha}{V_o} = 0.7 \cdot k_\alpha. \tag{15}$$

The screw conveyor capacity is determined by the following relation:

$$Q = \pi \psi_o \cdot V_{ax\alpha}\left(R_k^2 - R_c^2\right), \tag{16}$$

where $R_k$ – curvature radius of the pipeline.

The capacity of the screw conveyor with a changing transportation route is determined on the basis of the following relation:

$$N = Q \cdot L \cdot w, \tag{17}$$

where $w$ – specific power input for the transportation:

$$w = \frac{\mu_2 \cdot \rho \cdot R_c^2 \cdot \omega_f^2 \cdot \omega \cdot cos\,\beta}{V_f}, \tag{18}$$

where $L$ – length of transportation; $\omega_f$ – angular velocity of the section; $V_f$ – axial speed of material transportation by a hinged-sectional working body of a screw conveyor along a curved track; $\beta$ – is the angle of inclination of the material transportation trajectory.

The axial velocity and capacity of the bulk material transportation performed by the articulated-section operating device of the screw conveyor on the curved route have been determined.

For a flexible (sectioned) screw conveyor with a changing route, the elementary power is input for the transportation of the bulk material on an interval $dl$ and is determined by the following relation [18]:

$$dN = Q \cdot w(l)dl, \tag{19}$$

where $w(l) = \frac{\mu_2 \rho R_c^2 \omega \omega_f^2(l)\, cos[\beta(l)]}{V_f(l)}$.

In accordance with (1), the angular velocity of the flow is found by the following formula:

$$\omega_{f\alpha} = \omega - \frac{2\pi V_{ax\alpha}}{T_s}. \tag{20}$$

The inclination angle $\beta$ of the bulk material transportation trajectory is determined by the formula:

$$tan\,\beta = \frac{V_{ax\alpha}}{\omega_{f\alpha} R_c} = \frac{V_{ax\alpha}}{\left[\omega - \frac{2\pi V_{ax\alpha}}{T_s}\right] R_c}. \tag{21}$$

Axial speed of material transportation by a hinged-sectional working body of a screw conveyor with a curved track $V_f$ take equal $V_{ax\alpha}$.

Hence, the bulk material transportation capacity of the flexible (sectioned) screw conveyor with a changing transportation route is determined by the following relation:

$$N = Q \int_0^L w(l)dl = Q\mu_2 \rho R_c^2 \omega \int_0^L \frac{\left(\omega - \frac{2\pi V_{ax\alpha}}{T}\right)^2 cos\,\beta}{V_{ax\alpha}} dl. \tag{22}$$

It should be noted that $V_{ax\alpha}$, depends on the length of the transport, since $x$ is a horizontal projection $L$, i.e. length of transportation.

From the obtained analytical dependence (23), it can be seen that with an increase in the angle $\beta$ of inclination of the material transportation trajectory, the values of the energy-power parameters of this screw conveyor increase, and an increase in the pitch of the screw turns in the direction of material movement leads to a decrease in the energy-power parameters of transportation.

In the ball joint drive, the same as in case of the universal-joint drive, the swivel joint transfers the rotary motion with certain non-uniformity, which is caused by the shift of the sections with respect to each other due to the motion of the balls.

The basic fixed coordinate system $Oxyz$ is chosen as follows. Its origin $O$ is placed at the centre of the swivel joint, the axis $Ox$ is aligned with the centreline of the first section, the axis $Oz$ is aligned with the axis of rotation with respect to the first section (Fig. 2). Accordingly, the rotated (by an angle of $\alpha$) coordinate system has its axis $O'x'$ aligned with the centreline of the second section, its axis $O'z'$ is aligned with the axis $Oz$.

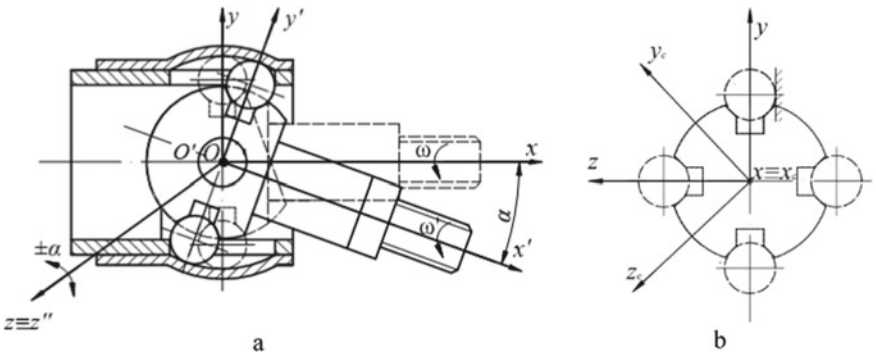


**Fig. 2** Schematic model of swivel-joint drive: **a** – side view; **b** – front view

Additionally, for each section its own couple of coordinate systems is assigned – $O_c x_c y_c z_c$ and $O_c' x_c' y_c' z_c'$, which are rigidly connected with the respective sections and at the initial instance $t = 0$ coincide with the above-mentioned basic and rotated coordinate systems.

For the transition from one coordinate system to the other, the homogeneous coordinate systems $Oxyz1$, $O'x'y'z'1$, $O_c x_c y_c z_c 1$, $O_c' x_c' y_c' z_c' 1$ are used.

Hence, the rotation of one section $(O_c' x_c' y_c' z_c')$ in the basic coordinate system $Oxyz$ about the axis $Ox$ can be represented in the matrix form as follows:

$$\begin{pmatrix} x \\ y \\ z \\ 1 \end{pmatrix} = \begin{pmatrix} cos(\omega t) & -sin(\omega t) & 0 & 0 \\ sin(\omega t) & cos(\omega t) & 0 & 0 \\ 0 & 0 & 1 & 0 \\ 0 & 0 & 0 & 1 \end{pmatrix} \begin{pmatrix} x_c \\ y_c \\ z_c \\ 1 \end{pmatrix} \tag{23}$$

In the coordinate system $O_c x_c y_c z_c$, the equation of the working surface of the upper slot is as follows:

$$-z_c - r = 0, \tag{24}$$

where $r$ – radius of the ball (half of the slot width).

In the basic coordinate system, the equation of the rotating surface of the slot is as follows:

$$y\, sin(\omega t + \varphi_i) - z\, cos(\omega t + \varphi_i) - r = 0, \tag{25}$$

where $\varphi_1 = 0$ for the upper slot, $\varphi_i = \frac{\pi}{2}(i - 1)$ for the slot of the following $i$-th ball.

The rotation of the coordinate system $O_c' x_c' y_c' z_c'$ relative to the rotated coordinate system $O_c x_c y_c z_c$ is described by the similar relation (23).

Accordingly, the $i$-th ball will have the following current coordinates of its centre in the coordinate system $O'x'y'z'$:

$$C_i' \left\{ x_{ci}' = 0;\ y_{ci}' = R\, cos(\omega' t + \varphi');\ z_{ci}' = sin(\omega' t + \varphi') \right\}.$$

The relation between the system $Oxyz$ and the rotated coordinate system $O'x'y'z'$ in the matrix form is determined by the rotation of the second section through the angle (-$\alpha$) (acc. to Fig. 2).

Accordingly:

$$\begin{pmatrix} x \\ y \\ z \\ 1 \end{pmatrix} = \begin{pmatrix} cos\,\alpha & sin\,\alpha & 0 & 0 \\ -sin\,\alpha & cos\,\alpha & 0 & 0 \\ 0 & 0 & 1 & 0 \\ 0 & 0 & 0 & 1 \end{pmatrix} \begin{pmatrix} 0 \\ R\, cos(\omega' t + \varphi') \\ R\, sin(\omega' t + \varphi') \\ 1 \end{pmatrix} \tag{26}$$

In the fixed coordinate system $O'x'y'z'$, the current coordinates of the balls rolling together with the second section are:

$$\begin{aligned} x_{ci} &= R\,sin\,\alpha\,sin(\omega' t + \varphi_i^{'}); \\ y_{ci} &= R\,cos\,\alpha\,cos(\omega' t + \varphi_i^{'}); \\ z_{ci} &= R\,sin\,\alpha\,cos(\omega' t + \varphi_i^{'}). \end{aligned} \tag{27}$$

The next step is to break provisionally the kinematic link between the sections and allow each of them to move independently with the same angular velocity: $\omega' = \omega$.

In that case, the coordinates of the ball centres will be described by the relations (27) at $\omega' = \omega$, $\varphi' = \varphi$, their distances from each of the flat surfaces of the slots are determined by means of substituting their coordinates into the Eq. (25):

$$l = |R\,cos\,\alpha\,cos(\omega t + \varphi_i)sin(\omega t + \varphi_i) - R\,sin\,\alpha\,cos(\omega t + \varphi_i) - r|. \tag{28}$$

It is obvious that at $t = 0$, $l = r$, that is, ball 1 touches the surface of the slot. Also, due to the smallness of the angle $\alpha$, we can take $sin\,\alpha \approx sin(\omega t + \varphi_i)$.

The expression (28) can be transformed as follows:

$$\begin{aligned} l =& |R(cos\,\alpha - 1 + 1)cos(\omega t + \varphi_i)sin(\omega t + \varphi_i) - R\,sin(\omega t + \varphi_i) \\ & cos(\omega t + \varphi_i) - r| \\ =& |R(cos\,\alpha - 1)cos(\omega t + \varphi_i)sin(\omega t + \varphi_i) - r| \\ =& \left| \frac{R\,sin[2(\omega t + \varphi_i)](1 - cos\,\alpha)}{2} + r \right|. \end{aligned} \tag{29}$$

At the current instance $t$, the ball in the broken kinematic link lags behind the surface of the slot by the following amount:

$$\Delta l = l - r = \frac{R\,sin[2(\omega t + \varphi_i)](1 - cos\,\alpha)}{2} \tag{30}$$

The analysis of the relation (25) indicates that at the instance, when $\varphi_1 = 0$, $\varphi_2 = \frac{\pi}{2}$, $\varphi_3 = \pi$, $\varphi_4 = \frac{3\pi}{2}$, there is no clearance between the ball and the surface of the slot. However, the clearance in the intermediate states results in the following angular deviation $\Delta\varphi$ of the ball:

$$\Delta\varphi = arcsin\{(1 - cos\,\alpha)sin[2(\omega t + \varphi_i)]\}.$$

Respectively, when the kinematic link is closed, the second section will be displaced relative to the first one through the following angle of rotation:

$$\omega' t + \varphi_i^{'} = \omega t + \varphi_i - \Delta\varphi.$$

Thus, the angular velocity of the next section is determined by the following relation:

$$\omega' = \omega - \frac{\Delta\varphi}{t} = \omega - \frac{arcsin\{(1 - cos\,\alpha)sin[2(\omega t + \varphi_i)]\}}{t}. \tag{31}$$

The analysis of the relation proves that the angular velocities of the adjacent sections are almost equal to each other.

In order to carry out experimental research into the performance of the screw conveyors in the transportation of agricultural materials, a test unit of the combined screw conveyor has been developed. The unit comprises the loading pipeline 1 and the discharge pipeline 2, as shown in Fig. 3a. They are made in the form of closed casings 3 and 4 with round cross-sections, in which the helical spirals 5 and 6 are installed. The helical spirals are connected to the drive shafts 7 and 8 of the motors 9 and 10.

In the area of the drive shafts, the pipelines are connected with each other via the two Sects. 11 and 12 of the transfer pipe. Each section is connected at one end to the opening in the closed casing 3 or 4, respectively, their other ends are connected with each other. The helical spirals are installed so that their centrelines coincide with the axes of the motor drive shafts. The pipelines in the area of their connection by the transfer pipe sections can be positioned as in the horizontal plane (Fig. 3b), so in the vertical one (Fig. 3c).

In the course of operation, the bulk material is fed into the intake area of the loading pipeline, then the spiral 5 in the casing transports it towards the transfer

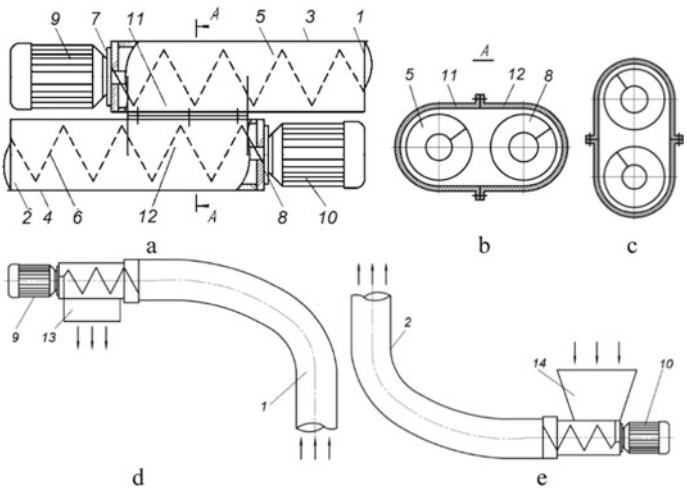


**Fig. 3** Schematic model of flexible screw conveyor: **a** – general view; **b** – horizontal arrangement of pipelines; **c** – vertical arrangement of pipelines; **d** – single pipeline alternative of loading conveyor; **e** – single pipeline alternative of discharge conveyor

pipe. Thereafter, the material from the transfer pipe is transferred onto the spiral 6 and transported to the discharge area.

The conveyor can also be operated as a single pipeline. In that case, the transfer pipe sections are equipped with respective special devices: discharge window 13 is installed on the loading pipeline, loading hopper 14 – on the discharge pipeline.

In the first case, the single pipeline conveyor operates in the intake or loading mode (Fig. 3d), in the second case – in the feeding or discharge mode (Fig. 3e).

During the experiments, the bulk agricultural material is fed from the hopper into the loading pipeline, the operating device transports it to the transfer pipe of the test unit, then the operating device in the discharge pipeline carries it to the discharge area.

For the analysis of the obtained results, the graphic relations have been plotted between the torque $T$ and the motor capacity $N$, on the one hand, and the operating device rotation frequency $n$, on the other hand, at different values of the bulk material lifting height $h$ and the process pipeline curvature radius $R_k$. The peak (maximum) values of the data obtained in the experiments have been used for plotting the diagrams.

In the experiments, the values of torque and motor capacity were recorded as percentage of the nominal ratings. The motor capacity was determined as the product of the motor power rating (2.2 kW) and the value for the selected mode of operation. The same was applied to the torque.

The experimental investigations were carried out with the use of the 3.5 m long material transportation pipeline. Wheat grain, peas and commercial salt were used as the bulk material.

## 3 Results and Discussion

Basing on the results of the completed experiments, the graphic relations have been plotted that show how the values of torque $T$ and capacity $N$ change with the operating device drive shaft rotation frequency, in case the process pipeline is fully filled with bulk agricultural material (Fig. 4).

The analysis of the graphic relations has proved that a rise in the operating device rotation frequency $n$ from 300 to 600 rpm results in the reduction of the torque $T$, the decrease is $\Delta T = 7.4\%$ for wheat grain, for commercial salt $\Delta T = 5\%$.

As regards the capacity $N$, the relation shows a rather clearly marked trend of the linear growth of $N$ with the increase of the operating device rotation frequency. For example, in case of wheat grain $\Delta N = 54\%$, in case of commercial salt $\Delta N = 59\%$.

Also, experimental research has been carried out with a purpose of determining the effect of changes in the material lifting height $h$ and process pipeline curvature radius $R_k$ on the values of the torque $T$ and capacity $N$ of the conveyor drive, when transporting commercial salt, wheat and peas.

In view of the fact that in the previous research the effect of changes in the operating device rotation frequency on the value of the torque was analysed in detail,

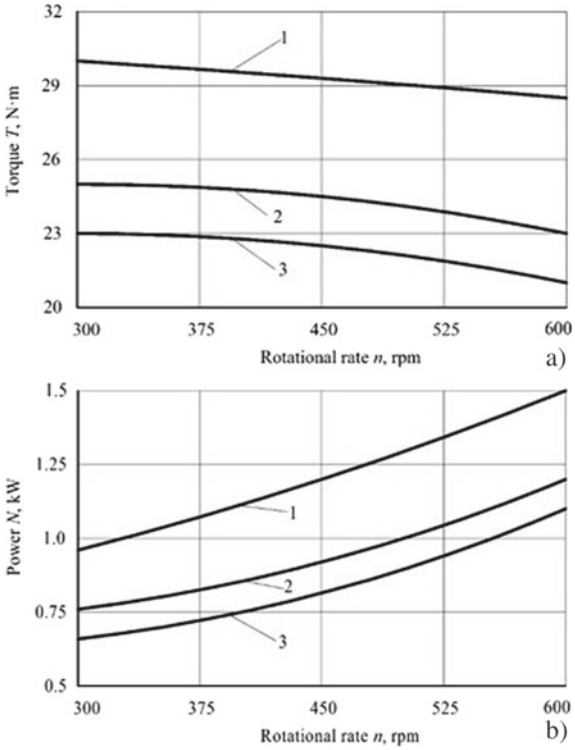


**Fig. 4** Graphic relations between torque $T$ **a** and power $N$ **b** and operating device rotation frequency n: 1 – commercial salt; 2 – peas; 3 – wheat

in the described experiments the operating device rotation frequency was maintained constant, its value was equal to 450 rpm.

Using the results of the experimental research, the graphic relations have been plotted between the value of the torque output by the drive of the articulated-section screw operating device, on the one hand, and the height $h$ of the material motion path (Fig. 5a) and the curvature radius $R_k$ of the process pipeline (Fig. 5b), on the other hand.

The analysis of the diagrams (Fig. 5a) indicates that an increase in the process pipeline curvature radius $R_k$ from 0.6 to 1.8 m results in the reduction of the torque $T$, the decrease $\Delta T$ is equal to 14% for wheat grain, for peas $\Delta T = 13\%$, for commercial salt $\Delta T = 10\%$.

The analysis of the graphic relations (Fig. 5b) has proved that an increase in the height of the bulk material motion path from 0.3 to 1.7 m brings about a growth in the torque $T$, where the increase $\Delta T$ is equal to 25% for wheat grain, for peas $\Delta T = 30\%$, for commercial salt $\Delta T = 29\%$.

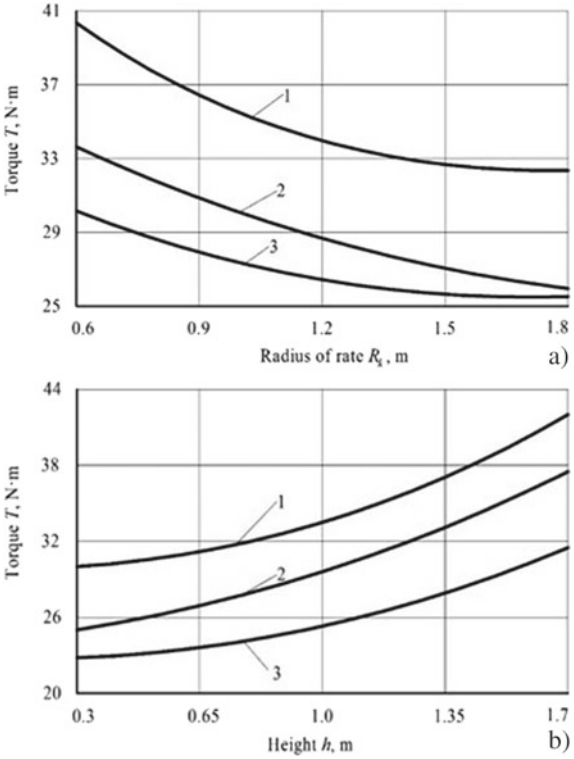


**Fig. 5** Relations between torque $T$ imparted to operating device and process pipeline curvature radius $R_k$ **a** and material motion path height $h$ **b** at $n = 450$ rpm: 1 – commercial salt; 2 – wheat; 3 – peas

## 4 Conclusions

On the basis of the completed research into the power and load parameters of flexible screw conveyors, the graphic relations have been plotted that show, how the values of the torque $T$ and capacity $N$ change during the transportation of bulk material by a screw conveyor, when the conveyor operating device drive shaft rotation frequency changes, provided that the process pipeline is fully filled with grain material.

It has been established that an increase in the operating device rotation frequency $n$ from 300 to 600 rpm results in a decrease in the torque $T$, where the decrease $\Delta T$ is equal to 7.1% for wheat grain, 7.4% for peas, for commercial salt $\Delta T = 5\%$.

As regards the value of the capacity $N$, the obtained graphic relations show a rather clearly marked trend of its linear growth, when the operating device rotation frequency is increased. For example, in case of wheat grain $\Delta N = 50\%$, in case of peas $\Delta N = 54\%$, for commercial salt $\Delta N = 59\%$.

On the basis of the results of the completed research into the effect of changes in the curvature radius of the process pipeline with an articulated-section operating

device on the torque, it has been concluded that an increase in the process pipeline curvature radius $R_k$ from 0.6 to 1.8 м results in a decrease in the torque $T$. In case of wheat grain the decrease $\Delta T$ is equal to 14%, in case of peas $\Delta T = 13\%$, in case of commercial salt $\Delta T = 10\%$.

At the same time, it has been established that the torque $T$ increases, when the height, to which the bulk material is raised in its motion, is increased from 0.3 to 1.7 m. The torque increase $\Delta T$ is equal to 25% in case of wheat grain, for peas $\Delta T = 30\%$, for commercial salt $\Delta T = 29\%$.

## References


1. Hevko R, Vitrovyi A, Klendii O, Liubezna I (2017) Design engineering and substantiation of the parameters of sectional tools of flexible screw conveyers. Bull Transilvania Univ Brasov 10(59):39–46. Brasov, Romania
2. Lech M (2001) Mass flow rate measurement in vertical pneumatic conveying of solid. Powder Technol 114(1–3):55–58
3. Hevko RB, Klendiy MB, Klendiy OM (2016) Investigation of a transfer branch of a flexible screw conveyer. INMATEH Agric Eng 48(1):29–34
4. Rogatynska O, Liashuk O, Peleshok T, Liubachivskyi R (2015) Investigation of the process of loose material transportation by means of inclined screw conveyers. Bull I Pyliui Ternopil Natl Tech Univ 79:137–143. Ternopil/Ukraine
5. Bulgakov V, Pascuzzi S, Ivanovs S, Kaletnik G, Yanovich V (2018) Angular oscillation model to predict the performance of a vibratory ball mill for the fine grinding of grain. Biosyst Eng 171:155–164. https://doi.org/10.1016/j.biosystemseng.2018.04.021
6. Manetto G, Cerruto E, Pascuzzi S, Santoro F (2017) Improvements in citrus packing lines to reduce the mechanical damage to fruit. Chem Eng Trans 58:391–396. https://doi.org/10.3303/CET1758066
7. Bulgakov V, Pascuzzi S, Adamchuk V, Kuvachov V, Nozdrovicky L (2019) Theoretical study of transverse offsets of wide span tractor working implements and their influence on damage to row crops. Agriculture 9:144. https://doi.org/10.3390/agriculture9070144
8. Rohatynskyi RM, Diachun AI, Varian AR (2016) Investigation of kinematics of grain material in a screw conveyor with a rotating casing. Bull Kharkiv Petro Vasylenko Natl Tech Univ Agric 168:24–31. Kharkiv/Ukraine
9. Lyashuk OL, Rogatynska OR, Serilko DL (2015) Modeling of the vertical screw conveyer loading. INMATEH Agric Eng 45(1):87–94
10. Hevko RB, Rozum RI, Klendiy OM (2016) Development of design and investigation of operation processes of loading pipes of screw conveyors. INMATEH Agric Eng 50(3):89–94
11. Bulgakov V et al (2021) Study of the steering of a wide span vehicle controlled by a local positioning system. J Agric Eng LII:1144. https://doi.org/10.4081/jae.2021.1144
12. Bulgakov V, Pascuzzi S, Nadykto V, Ivanovs S, Adamchuk V (2021) Experimental study of the implement-and-tractor aggregate used for laying tracks of permanent traffic lanes inside controlled traffic farming systems. Soil Tillage Res 208:104895. https://doi.org/10.1016/j.still.2020.104895
13. Bulgakov V, Pascuzzi S, Ivanovs S, Nadykto V, Nowak J (2020) Kinematic discrepancy between driving wheels evaluated for a modular traction device. Biosyst Eng 196:88–96. https://doi.org/10.1016/j.biosystemseng.2020.05.017
14. Bulgakov V, Pascuzzi S, Adamchuk V, Ivanovs S, Pylypaka S (2019) A theoretical study of the limit path of the movement of a layer of soil along the plough mouldboard. Soil Tillage Res 195:104406. https://doi.org/10.1016/j.still.2019.104406

15. Bulgakov V, Pascuzzi S, Beloev H, Ivanovs S (2019) Theoretical investigations of the headland turning agility of a trailed asymmetric implement-and-tractor aggregate. Agriculture 9:224. https://doi.org/10.3390/agriculture9100224
16. Pascuzzi S, Anifantis AS, Santoro F (2020) The concept of a compact profile agricultural tractor suitable for use on specialised tree crops. Agriculture 10:123. https://doi.org/10.3390/agriculture10040123
17. Guerrieri AS, Anifantis AS, Santoro F, Pascuzzi S (2019) Study of a Large Square Baler with Innovative Technological Systems that Optimize the Baling Effectiveness. Agriculture 9(5):86. https://doi.org/10.3390/agriculture9050086
18. Bulgakov V, Pascuzzi S, Anifantis AS, Santoro F (2019) Oscillations analysis of front-mounted beet topper machine for biomass harvesting. Energies 12:2774. https://doi.org/10.3390/en12142774